Petroleum Science 23 (2026) 7487–7497

Contents lists available at ScienceDirect

Petroleum Science

journal homepage: www.keaipublishing.com/en/journals/petroleum-science

Original Paper

Catalytic pyrolysis of waste wind turbine blades using spent FCC catalysts for the production of phenol-rich oils

Hao-Lun Wang, Yue Ma, Zhi-Jun Fu, Lu Gong, Dong-Ling Xu, Ze-Kai Zhang, Jin-Ke Wang, Si-Jia Li, Feng-Zhi Guo, Chang-Tao Yue *

State Key Laboratory of Heavy Oil Processing, China University of Petroleum (Beijing), Beijing, 102249, China

ARTICLE INFO

Article history:
Received 4 December 2025
Received in revised form
26 January 2026
Accepted 12 May 2026
Available online 19 May 2026
Edited by Min Li
Handling editor: Xing-Ying Lan

Keywords:
Fluidized bed
Waste wind turbine blades
Spent FCC catalysts
Pyrolysis conditions
Yields and compositions of pyrolysates

ABSTRACT

The disposal of waste wind turbine blades and spent FCC catalysts represented two significant environmental challenges for the renewable energy and petroleum refining sectors, respectively. This study presented an integrated strategy for the synergistic conversion of these wastes by using catalytic pyrolysis in a fluidized-bed reactor. Using solid heat carriers and spent FCC catalysts, the influences of pyrolysis temperature, pyrolysis time, and blending ratio on yields and compositions of pyrolysates were systematically investigated. Under optimal conditions (550 °C, 20 min, blending ratio of 1:3), a high pyrolysis oil yield of 28.28 wt% was achieved. More importantly, GC-MS analysis revealed exceptional selectivity towards valuable chemicals with the content of phenolics in the pyrolysis oil reaching 91.07%, among which phenol accounted for 66.47%. The simultaneous production of pyrolysis gas was rich in light hydrocarbons and H_2. This work not only demonstrated a technically feasible "waste-to-resource" pathway for two industrial wastes but also provided a catalytic pyrolysis approach for selectively obtaining high-purity phenolic feedstocks from complex thermoset composites, providing new insights for sustainable waste management and chemical production.
© 2026 The Authors. Publishing services by Elsevier B.V. on behalf of KeAi Communications Co. Ltd. This is an open access article under the CC BY license (http://creativecommons.org/licenses/by/4.0/).

1. Introduction

The global transformation of the energy structure toward renewable sources, together with the green upgrading of traditional fossil-fuel industries, represented two major parallel themes in contemporary industrial development (Mavukwana et al., 2024). However, energy industry also produced large quantities of solid wastes with different characteristics causing environmental impacts (Xiang et al., 2025). In the petroleum refining industry, fluid catalytic cracking (FCC) units continuously produced much spent FCC catalysts, with a global cumulative rate as high as 2300 tons per day (Tian et al., 2022). Meanwhile, the development of the wind power industry has led to the generation of a substantial number of waste wind turbine blades (WWTB) (Ma et al., 2025; Teng et al., 2023). It was estimated that by 2050, the total global volume of WWTB would reach approximately 43 million tons (Liu and Barlow, 2017). Therefore, the development of simultaneously treating these two industry solid wastes and converting them into high-value products was not only crucial for environmental governance but also a key step toward advancing the circular economy and achieving industrial sustainability (Kabakcı and Şenlik, 2025; Lichtenegger et al., 2020).

FCC catalysts underwent deactivation due to coke deposition and metal poisoning. The global annual output of spent catalysts reached several million tons, and they were typically classified as hazardous waste (Liu et al., 2023; Wang et al., 2024). The dominant disposal treatment was landfill at the time, which essentially "transferred" the waste rather than "solved" it. However, it may pollute valuable land resources, impose substantial economic burdens on refineries and even pose potential environmental risks (Salvilla et al., 2025). Although metal recovery technologies existed, these methods tended to be costly, complex, and completely neglected the residual value of their catalytic structure of spent FCC catalysts (Mishra et al., 2025). These spent FCC catalysts were not completely deactivated, which typically retained considerable accessible surface area, pore structures, and acidic sites responsible for C–C bond cracking and isomerization (Marschall et al., 2025).

* Corresponding author.
E-mail address: yuect@cup.edu.cn (C.-T. Yue).
Peer review under the responsibility of China University of Petroleum (Beijing).

https://doi.org/10.1016/j.petsci.2026.05.017
1995-8226/© 2026 The Authors. Publishing services by Elsevier B.V. on behalf of KeAi Communications Co. Ltd. This is an open access article under the CC BY license (http://creativecommons.org/licenses/by/4.0/).

Wind turbine blades, with a service life of 20–25 years, were now approaching large-scale retirement. The WWTB were composed of glass-fiber/carbon-fiber reinforced thermoset resins, because of cross-linked chemically structures, the WWTB recycling had extremely challenge (Hamid et al., 2025; Xu et al., 2025). Mechanical shredding produced only low-value production (Wang et al., 2021; Xu et al., 2019); solvent-based recovery suffered from complex post-treatment, caused environmental pollution, and damage to glass fibers (Nistratov et al., 2022). In contrast, pyrolysis process decomposed the organic polymer resin into liquid fuels and valuable chemicals while allowing the recovery of reinforcing fibers nearly complete (Ekici et al., 2025). Chen et al. (2025) investigated the pyrolysis characteristics of WWTB and Py-GC/MS showed that the carbon chains of pyrolysis oil mainly contained C_9–C_{16} (48.97%–72.73%) including phenols, alcohols, ketones, and carboxylic acids. Ren et al. (2023) used photothermal pyrolysis to study the influence of temperature, heating rate, and gas flow on pyrolysate distribution and they found that bisphenol A (BPA) accounted for more than 40% of pyrolysis oil, and its pyrolysis oil increased with higher temperature, faster heating rate, and greater gas flow. Zhang et al. (2024) investigated the pyrolysis behavior of WWTB in a fixed-bed reactor, and analyzed the influence of atmosphere (N_2 or air) and temperature. The results showed that pyrolysis experiment under both N_2 and air produced different volumes of pyrolysis oil and gas, 450 °C was identified as the optimal pyrolysis temperature, and produced 13.17 wt% and 11.93 wt% of pyrolysis oil under N_2 and air, respectively. However, bio-oil obtained from direct pyrolysis contained high oxygen content, strong acidity, and poor thermal stability; its corrosiveness and low quality made it unsuitable for direct use as a fuel or chemical feedstock. Catalytic pyrolysis was effective method for upgrading the oil quality. In order to catalytic pyrolysis waste, the experiment required an efficient cracking and deoxygenation catalyst (Li et al., 2025; Lu et al., 2020). The ideal catalyst needed to possess sufficient acidity to crack macromolecules and remove oxygen, while also being economically viable for waste-treatment applications. The spent FCC catalysts with abundant Brønsted and Lewis acid sites had active centers for cracking and deoxygenation, and hierarchical pore networks conducive to the diffusion and transformation of large molecules. These characteristics were advantageous, especially the spent FCC used lower cost to treat waste (Kongngoen et al., 2023; Liu et al., 2023). Therefore, this manuscript proposed an innovative waste-to-resource strategy, utilizing spent FCC catalysts from petroleum refineries for the catalytic pyrolysis of WWTB to achieve resource utilization of both solid wastes.

Because of residual catalytic potential of spent FCC catalysts, researchers have begun exploring their application in catalytic pyrolysis of various waste. Aisien et al. (2021) investigated the process characteristics of waste polypropylene (WPP) catalytic pyrolysis by spent FCC catalysts in a batch reactor. They found that the catalyst significantly improved the fuel properties, achieving a heating value of 47.3 MJ/kg (approaching diesel standards), and notably improved aromatic content; the maximum liquid yield of 70.5% occurred at 400 °C with 7.5 wt% catalyst. Kanduri and Seethamraju (2023) investigated the co-pyrolysis of peanut shells and polypropylene (PP) using spent FCC catalysts. The result was shown that the spent FCC catalysts increased oil yields, reduced char formation, and increased gas yield. The catalysts efficiently cracked PP into short-chain olefins ($<C_{10}$), with C_9 as the dominant product. Kongngoen et al. (2023) investigated the upgrading of heavy pyrolytic waxes derived from mixed plastics (HDPE, LDPE, and PP) using various catalysts (spent FCC, HY zeolite, and MCM-41) in a fixed-bed reactor, showing that spent FCC performed best in increasing liquid yield (74.2%) while minimizing coke deposition (6.8%). Mishra et al. (2025) investigated microwave-assisted catalytic pyrolysis of low-density polyethylene (LDPE) using spent FCC catalysts. The optimal pyrolysis temperature was 450 °C, producing liquid hydrocarbons in the C_8–C_{30} range, suitable for gasoline and diesel fractions, and gas yield reached up to 90 wt% under optimal condition. Although spent FCC catalysts increased oil yields and cracked macromolecules into smaller fragments, the pyrolysis behavior and product distribution of wind turbine blade composites were different from polyolefin plastics.

These studies confirmed that spent FCC catalysts increased pyrolysis oil yield and improved product quality, particularly by promoting the production of high-value fuels like diesel and gasoline. However, limitations were identified, including concerns about coke formation, especially when used with mixed plastics. Furthermore, despite good results obtained from small-scale batch reactors, research on their performance in fluidized-bed reactors, which better represented industrial-scale processes was remained limited. Fluidized-bed reactors offered several advantages for catalytic pyrolysis, including improved heat and mass transfer, more uniform temperature control, and the capacity to handle larger quantities of feedstock. These characteristics enabled more efficient and scalable reactions, which were particularly critical for industrial applications requiring continuous operation and high throughput. Additionally, the pyrolysis behavior of composites with high epoxy resin content, such as WWTB could not be effectively addressed by spent FCC catalysts, as their behavior differed significantly from that of polyolefins. Thus, further investigations were necessary to optimize the performance of the catalysts for a broader range of waste materials and reactors that more closely simulated industrial conditions.

This manuscript aimed to evaluate the feasibility and optimization pathway for co-processing spent FCC catalysts and WWTB. First, the spent FCC catalysts were comprehensively characterized to quantify their residual catalytic potential. Next, the pyrolysis parameters of a fluidized-bed reactor were investigated to determine their influence on yields of pyrolysis gas, pyrolysis oil, and solid residue. The composition of the pyrolysis oil was analyzed, and indicated it had high selectivity towards phenolic compounds, especially phenol. This work not only presented a concrete technological solution but also provided theoretical foundations and experimental evidence for cross-industry collaborative high-value recovery of solid wastes.

2. Materials and methods

2.1. Experimental materials

WWTB sample was from China National Energy Group, which have been retired after 20 years of service. The manufacturer was Sinoma science and technology corporation, and epoxy resin was the base resin. The WWTB sample was crushed to a particle size of less than 0.3 mm, which was composed of 60% glass fiber, 35% resin, 5% core materials, and structural adhesive. The spent FCC catalysts came from Sinopec Yanshan Petrochemical Company and were applied in fluidized bed experiments after being activated at 700 °C for 5 h.

2.2. Characteristics of spent FCC catalysts and WWTB

In this study, in order to ensure the rigor and repeatability of the fluidized bed catalytic pyrolysis experiments of WWTB, before starting all the experiments, WWTB powder was powdered to less than 0.3 mm and dried in an electric blast

drying oven for 24 h. Industrial analysis of WWTB powder was conducted using a muffle furnace (SRJX9) and an Electrothermal blast drying oven (DHG-9070A) according to GB/T 212-2008. Elemental analysis was performed using an elemental analyzer in accordance with GB/T 31391-2015 standards for experiments. The TG experiments used a DTA-TG-DTG analyzer (Supporting Information, Text S1). The pyrolysis gas composition was analyzed by GC (Supporting Information, Text S2), and the Pyrolysis oil composition was analyzed by GC-MS (Supporting Information, Text S3). The individual peak areas detected were quantified using the area normalization method.

2.3. Pyrolysis experiments using a fluidized bed reactor

This pyrolysis experiment was conducted using a fluidized bed reactor, as illustrated in Fig. 1. The spent FCC catalysts were used as a solid heat carrier and were weighed and pre-loaded into the reactor. After connecting gas lines and inserting thermocouples, the PID temperature program and condensation unit were activated at −20 °C. Once the temperature stabilized, the system was purged with high-purity N_2 at a flow rate of 0.5 L/min for 5 min to remove any remaining air. Pre-weighed waste wind turbine blade powder ($m_w = 10.0 \pm 0.1$ g) was then fed into the preheated zone at the target temperature under N_2 fluidization. After the pyrolysis process lasted for 20 min, the temperature program was stopped. Then, the solid residue was collected, and the pyrolysis gas volume was measured by water displacement for GC analysis. The pyrolysis oil was weighed as m_{oil} and subjected to GC-MS analysis. Based on the GC results, the pyrolysis gas mass is calculated as m_{gas}. The yields of pyrolysis oil, pyrolysis gas, and solid residue were obtained by dividing the weight of the pyrolysis oil, pyrolysis gas, and solid residue by the weight of the raw materials, respectively.

The yield of pyrolysis oil ($Yield_{oil}$), gas + loss ($Yield_{gas+loss}$), and solid residue ($Yield_{solid}$) were calculated on a mass basis according to the following equations:

$$Yield_{oil}\ (wt\%) = \frac{m_{oil}}{m_w} \quad (1)$$

$$Yield_{soild}\ (wt\%) = \frac{m_{soild}}{m_w} \quad (2)$$

$$Yield_{gas+loss}\ (wt\%) = 1 - Yield_{oil} - Yield_{soild} \quad (3)$$

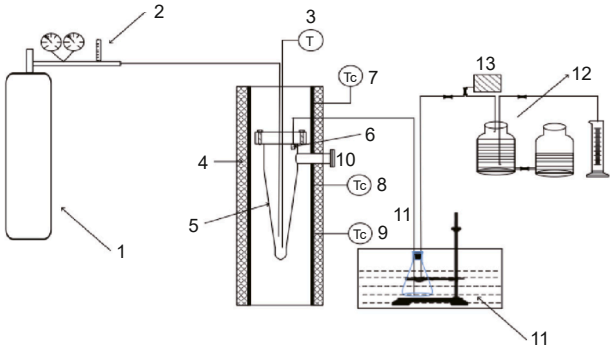


Fig. 1. Fluidized bed device diagram. Note: (1) Nitrogen bottle, (2) rotor flow meter, (3) thermocouple temperature measurement, (4) Kelvin heating furnace, (5) fluidized bed reactor, (6) outlet filter, (7) upper section temperature control, (8) middle section temperature control, (9) lower section temperature control, (10) solid inlet, (11) condensation device, (12) drainage gas collection device, (13) gas bag.

3. Results and discussion

3.1. Characteristics of catalysts

Based on the characteristics of the spent FCC catalyst before and after activation, as shown in Table 1 and Fig. 2(a and b), it can be observed that the activation treatment effectively removed the carbon deposits obstructing the pore channels, not only increased the catalyst's surface area and total pore volume but also increased the mesopore volume in the 3–4 nm range and slightly enlarged the average pore size. These improvements led to the establishment of more unobstructed mass-transfer pathways. As shown in Fig. 2(a and b), these improvements of pore structure were demonstrated by the overall upward shift of the isotherm, and the pronounced expansion of the hysteresis loop confirmed the optimization of the mesoporous structure and the improvement of pore accessibility (Li et al., 2024).

The activation treatment led to a significant recovery of the catalyst's acidic functionality, as evidenced by NH_3-TPD analysis in Fig. 2(c). A significant increase in the intensity of the high-temperature desorption peak (>400 °C), associated with strong acid sites, indicated the effective restoration of active centers critical for cracking refractory hydrocarbons. Concurrently, a notable expansion of the area under the NH_3-TPD curve reflected a significant increase in the total acid site concentration.

The active components of the spent FCC catalyst are mainly Y-type zeolite molecular sieves. The XRD patterns Fig. 2(d) showed that both samples retained the characteristic FAU-type diffraction peaks, indicating that the catalyst framework remained intact during activation (de la Puente et al., 2002). After activation, the peak intensities increased, while the background signal decreased, reflecting the effective removal of carbonaceous and metallic deposits that had previously suppressed crystallinity. The enhanced low-angle reflections further confirm that the FAU microporous structure was well preserved and more fully exposed.

The prolonged high-temperature operating environment led to the destruction of more Lewis acid sites. Although the total acid amount remained at a medium level after activation, the high-temperature degradation limited the extent of damage to the Y-type zeolite structure. After activation, the Y-type zeolite structure of the spent FCC catalysts provided a substantial number of Brønsted acid sites, transforming the spent FCC catalysts into one dominated by Brønsted acid sites. These Brønsted acid sites effectively cleaved C–C and C–O bonds, converted the epoxy resin into phenolic compounds. The reduction in the total acid amount inhibited further deep cracking of the phenolic products.

3.2. Characteristics of WWTB

3.2.1. Industrial analysis and elemental analysis of WWTB

Elemental analysis and industrial analysis of WWTB were conducted, and the results were shown in Table 2. It was observed that the WWTB sample had a high percentage of ash. This was due to the fact that the glass fibers were not involved in the pyrolysis reactions; therefore, most of the ash consisted of glass fiber. The volatile matter accounted for 29.88%, indicating that the pyrolysis process would produce a large amount of pyrolysis oil and pyrolysis gas, with significant pyrolysis recovery potential. The elemental analysis results of WWTB shown in Table 3 indicated that the WWTB sample contained high levels of carbon (19.92 wt%), sulfur (5.94 wt%), and hydrogen (2.47 wt%), suggesting that the material was primarily composed of sulfur-containing organic or polymeric substances. The low levels of oxygen (0.92 wt%) and nitrogen (0.12 wt%) further supported the

Table 1
BET surface area, pore volume, and pore size of the catalysts.

Sample	S_{BET}, m^2/g	Pore volume, cm^3/g	Pore size, nm
Spent FCC catalysts	96.89	0.083	7.41
Activated spent FCC catalysts	100.05	0.084	7.84

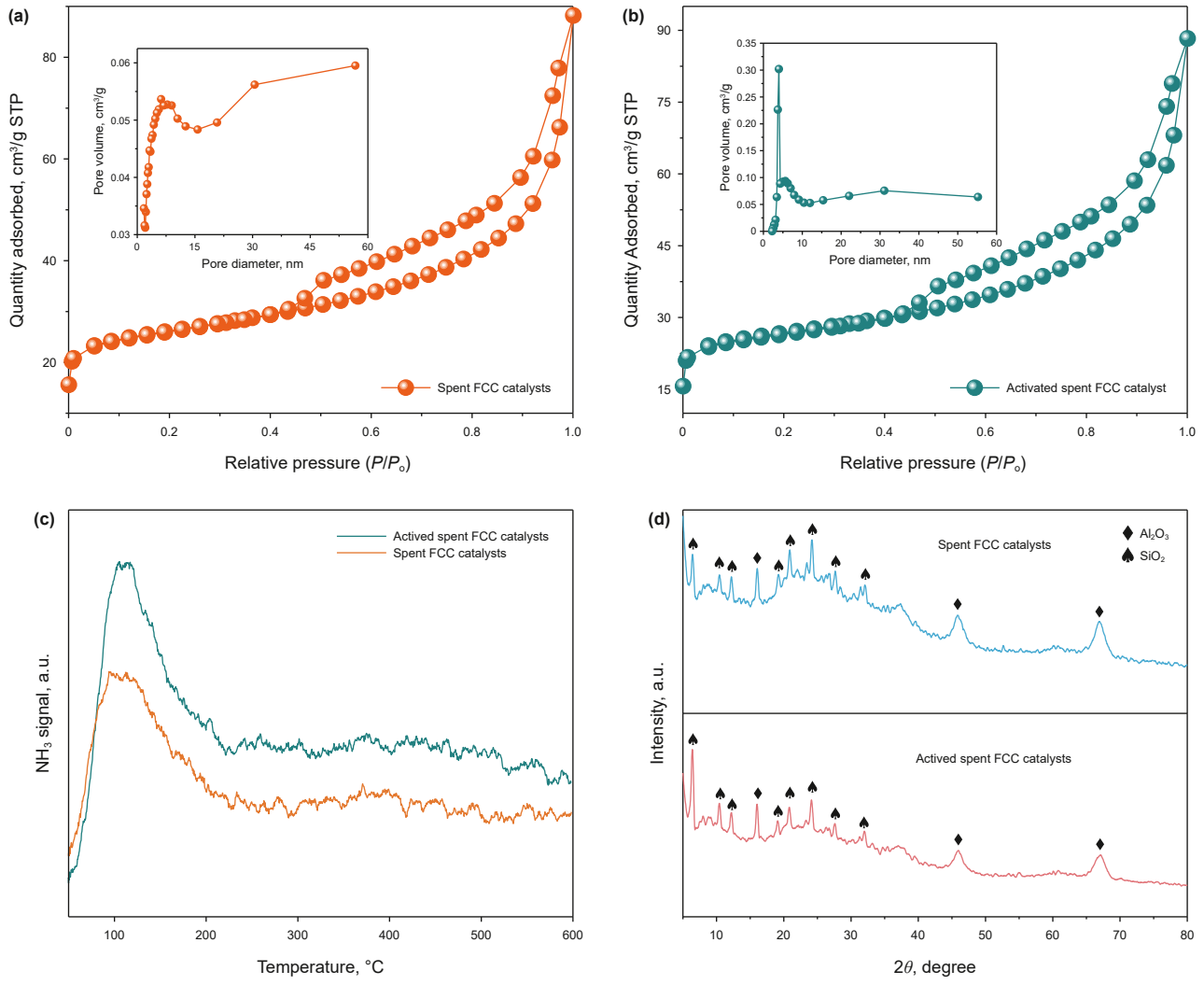


Fig. 2. Characteristics of catalysts. **(a)** N_2 adsorption-desorption isotherms, **(b)** pore size distribution profiles, **(c)** NH_3-TPD profiles, **(d)** XRD patterns.

Table 2
Industrial analysis of WWTB.

Surface water	Ash	Volatile matter	Fixed carbon
0	69.30	29.88	0.83

Table 3
Elemental analysis of WWTB.

Element name	Content
C	19.92
H	2.47
O	0.92
N	0.12
S	5.94

conclusion that the material likely consisted of a thermosetting resin or composite material.

3.2.2. FTIR analysis of WWTB sample

The FTIR spectrum of the WWTB sample was shown in Fig. 3(a). The results showed that stretching peaks appeared at 3836 and 3748 cm^{-1}, which might be caused by the interference of water vapor generated by pyrolysis (Gu et al., 2013). A stretching peak appeared at 3659 cm^{-1}, which might be the –OH absorption peak in phenol. A sharp absorption peak appeared at 2951 cm^{-1}, which

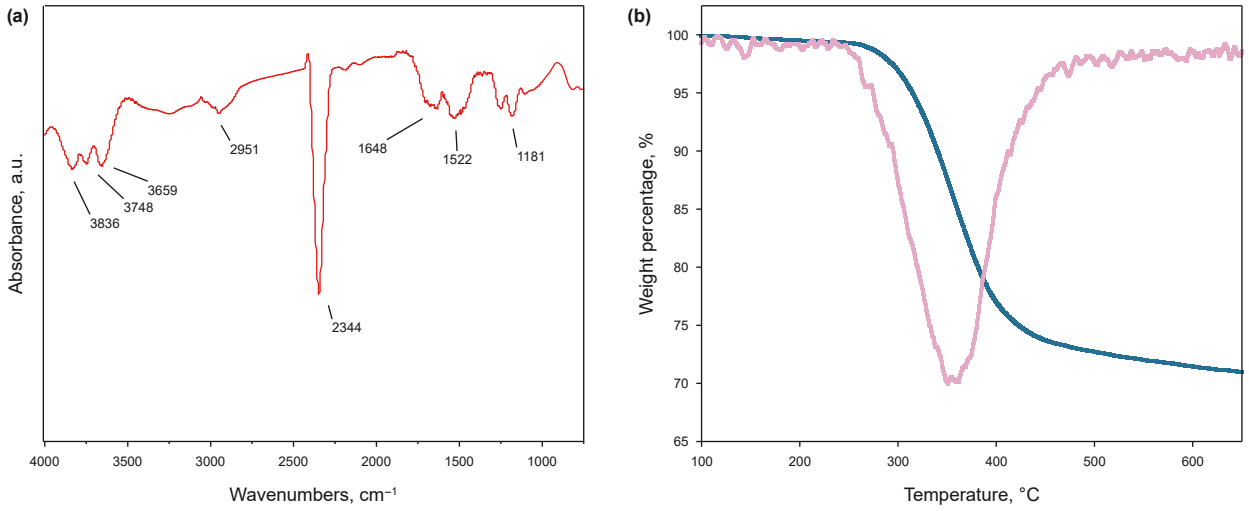


Fig. 3. Characteristics of WWTB. **(a)** The FTIR spectrum, **(b)** the TG curves and DTG curve.

might be the C–H absorption peak in aromatic compounds. A sharp absorption peak also appeared at 2344 cm^{-1}, which might be the CO_2 absorption peak caused by the increase in temperature. Stretching vibration peaks at 1648 and 1522 cm^{-1} might be the absorption peaks of C=C and C–C in the aromatic ring. There was a stretching vibration peak at 1180 cm^{-1}, which might be the C–O–C absorption peak (Choi et al., 2024).

3.3. Thermogravimetric analysis of WWTB

The TG and DTG curves of the WWTB sample at 15 °C/min heating rate were shown in Fig. 3(b), and the results showed that the pyrolysis weight loss was mainly concentrated in the range between 260 and 500 °C. At pyrolysis temperatures above 550 °C, this stage accounted for about 1% of the thermogravimetric weight loss, and most of the volatile components had already disappeared at lower temperatures. According to the DTG curve results, it could be seen that the maximum weight loss rate occurred at 345 °C, and fluctuations occurred at the front and rear ends of the curve because the glass fibers in the WWTB did not participate in the pyrolysis reaction. Based on the thermogravimetric analysis results, in order to explore the optimal pyrolysis temperature to achieve high yields of pyrolysis oil, 400, 450, 500, and 550 °C were set as the temperatures examined in the following research.

3.4. Influence of pyrolysis conditions on the yields of pyrolysates

3.4.1. Influence of solid heat carrier

When the pyrolysis temperature was 550 °C, the gas velocity was 0.5 L/s, the reaction time was 20 min, the blending ratio of WWTB to solid heat carrier was 1:2, and the influence of different solid heat carriers on the yields of pyrolysates was determined, and the results were shown in Fig. 4(a). When the solid heat carrier was changed from quartz to spent FCC catalysts and activated spent FCC catalysts, the yield of pyrolysis oil increased from 18.03 to 19.69 wt% and 23.32 wt%, the yield of gas and loss increased from 15.94 wt% to 19.47 wt% and 29.31 wt%, and the yield of solid residue decreased from 66.03 to 60.9 wt% and 47.37 wt%. Spent FCC catalysts were mainly composed of zeolite molecular sieves, which also had a large number of Brønsted acidic sites. The protons provided by the Brønsted acid (H^+) would convert the olefins and hydroxyls generated in the pyrolysis process into saturated hydrocarbons and H_2O, and could selectively broke the ether bonds (C–O–C) in the epoxy resin, thereby promoting the pyrolysis of the epoxy resin macromolecules and resulting in a significant decrease in the yield of solid residue (Wang et al., 2023). At the same time, the spent FCC catalysts promoted the cracking of C–C bonds and intermediate products (such as the cracking of bisphenol A to produce CH_4, C_2H_4, and other short-chain hydrocarbons) in the epoxy resin, which led to a significant increase in the yield of pyrolysis gas and loss. The activated spent FCC catalyst further promotes cracking of WWTB due to the elevated acid content, resulting in a further increase in the yields of pyrolysis oil and pyrolysis gas (Passamonti and Sedran, 2012).

3.4.2. Influence of pyrolysis temperature

When the gas velocity was 0.5 L/s, the activated spent FCC catalysts were used as the solid heat carrier, the blending ratio of WWTB to solid heat carrier was 1:2, and the reaction time was 20 min. The influence of pyrolysis temperatures on the yields of pyrolysates was investigated, and the results were shown in Fig. 4(b). It was observed that as the reaction temperature increased from 400 to 550 °C, the yield of pyrolysis oil increased from 14.15 to 23.32 wt%, the yield of solid residue decreased from 55.56 to 47.36 wt%, and the yield of pyrolysis gas and loss slightly decreased from 34.07 to 29.31 wt%. It could be seen that pyrolysis temperature affected the heat transfer efficiency of the pyrolysis process and the intensity of the organic matter involved in the reactions. With the increase in temperature, the C–O and C–C bonds in the main and side chains of the epoxy resin matrix were promoted to fracture, generating pyrolysis oil and pyrolysis gas. When the pyrolysis temperature reached 550 °C, the higher temperature triggered further pyrolysis of coatings and heat-resistant components between different structural parts of the WWTB, resulting in the highest yield of 23.32 wt% of pyrolysis oil. When the temperature reached 600 °C, secondary reactions of pyrolysis oil occurred, leading to an increase in the yield of pyrolysis gas and loss. According to the results of the thermogravimetric analysis shown in Fig. 3(b), the pyrolysis reactions were basically completed at 550 °C, which was consistent with the yield of solid residue did not change significantly between 550 and 600 °C.

3.4.3. Influence of pyrolysis time

When the pyrolysis temperature was selected as 550 °C, the gas velocity was 0.5 L/s, the activated spent FCC catalysts was used as the solid heat carrier, and the blending ratio of the WWTB to the solid heat carrier was 1:2, the effects of different pyrolysis

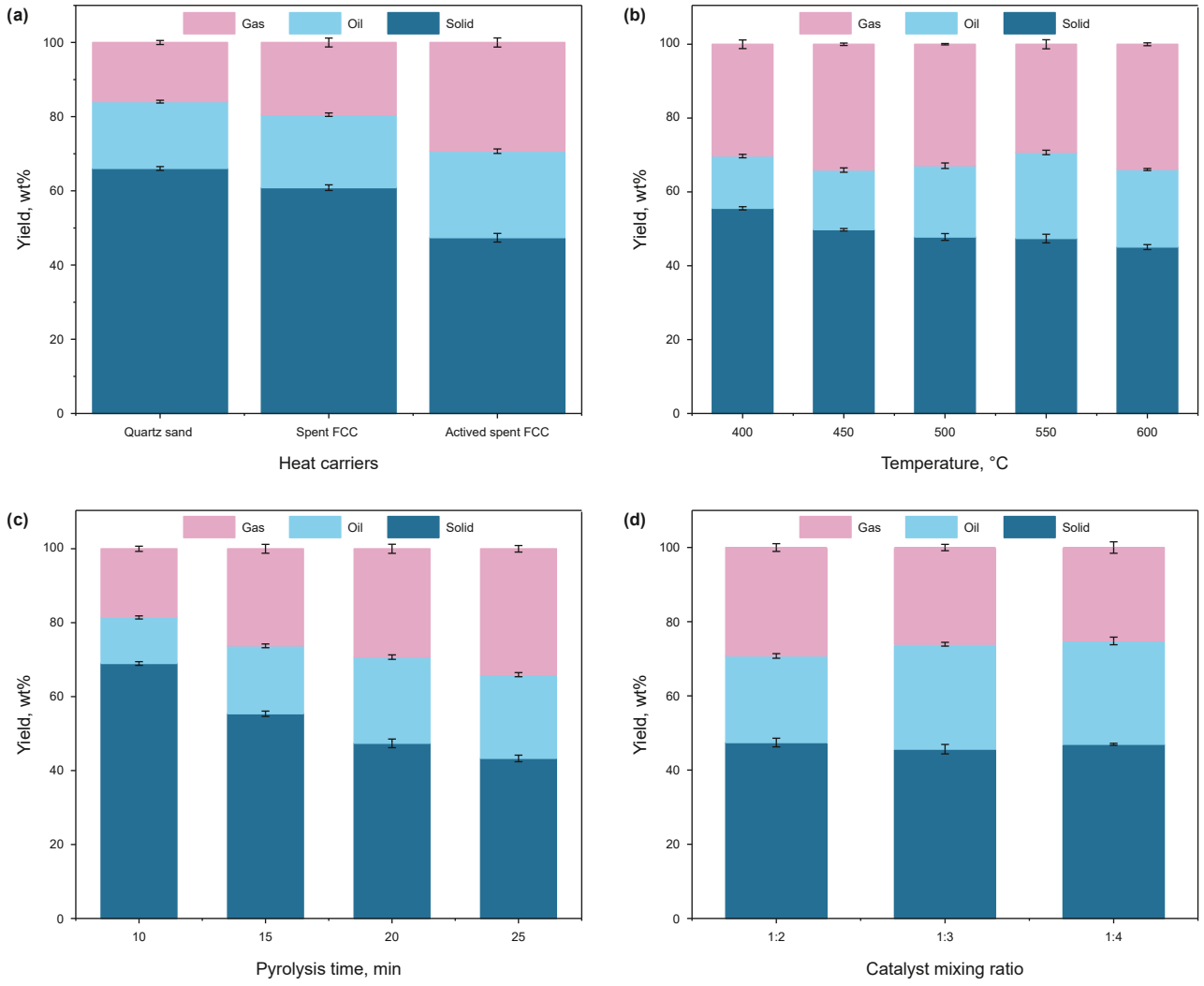


Fig. 4. Influence of pyrolysis conditions on the yields of pyrolysates under different **(a)** heat carriers, **(b)** temperature, **(c)** pyrolysis time, **(d)** catalysts blending ratio.

times—10, 15, 20, and 25 min—on the yields of pyrolysates were investigated, and the results were shown in Fig. 4(c). As the pyrolysis time increased from 10 to 25 min, the yields of solid residue decreased from 68.98 to 43.33 wt%, the yields of pyrolysis oil increased from 12.45 to 23.29 wt%, and the yields of pyrolysis gas and loss increased from 18.57 to 34.07 wt%. The yield of solid residue changed significantly with pyrolysis time, which was attributed to the decomposition of epoxy resin. As a thermosetting material, epoxy resin underwent incomplete pyrolysis during a shorter time, where only the surface volatile components reacted. As the pyrolysis time increased, the pyrolysis process proceeded more completely, resulting in a significant reduction in the yield of solid residue. When the pyrolysis time reached 20 min, the yield of pyrolysis oil reached its maximum. Beyond 20 min, secondary reactions clearly led to a decrease in the yield of pyrolysis oil and an increase in the yield of pyrolysis gas.

3.4.4. Influence of blending ratio

When the pyrolysis temperature was 550 °C, the gas velocity was 0.5 L/s, the reaction time was 20 min, the activated spent FCC catalysts were used as the solid heat carrier, and the influence of the blending ratio of spent FCC catalysts and WWTB on the yield of pyrolysates was investigated, and the results were shown in Fig. 4(d). When the blending ratio was increased from 1:2 to 1:3, the yield of pyrolysis oil increased from 23.32 to 28.28 wt%, the yield of gas and loss decreased from 29.20 to 26.08 wt%, and the yield of solid residue decreased from 47.37 to 45.63 wt%. When the blending ratio was 1:3, the spent FCC catalysts were in full contact with the WWTB and promoted the cracking of epoxy resin macromolecules. When the blending ratio was 1:4, the larger amount of catalyst resulted in increased contact between pyrolysis oil and pyrolysis gas within the catalyst surface area, which caused excessive cracking of pyrolysis oil and led to a slight decrease in the yield of pyrolysis. It also caused excessive secondary reactions of the pyrolysis gas, resulting in a decreased yield of gas and loss. Therefore, the blending ratio of 1:3 was chosen to be the optimal pyrolysis condition.

3.5. Determination of the optimal process conditions

The yield of solid residue was significantly lower than the ash content of WWTB. This discrepancy was attributed to the operational characteristics of the fluidized-bed system. Specifically, pyrolysis experiments used piston feeding and N_2 fluidization. A part of WWTB powders and spent FCC catalysts were entrained by the gas flow which either captured by the top ceramic filter or lost from the system. Additionally, the spent FCC catalyst itself had a weight loss at the reaction temperature. The systematic mass losses were unavoidable in fluidized bed, and reduced some solid product.

Crucially, these systematic losses were consistent across all comparative experiment. Therefore, they did not affect the validity of the relative trends and mechanistic analysis discussed hereafter.

The optimal operating parameters were determined based on the highest pyrolysis oil yield. According to the experimental results, when the pyrolysis temperature was 550 °C, the pyrolysis time was 20 min, and the blending ratio of activated spent FCC catalysts was 1:3, the highest pyrolysis oil yield was 28.28 wt% under these optimized conditions, while the yields of pyrolysis gas and loss, and solid residue were 26.08 and 46.89 wt%, respectively. The spent FCC catalysts provided critical acidic active sites, improved the selective cleavage of epoxy resin bonds; the pyrolysis temperature of 550 °C ensured resin complete pyrolysis; the pyrolysis time of 20 min allowed sufficient duration for thorough depolymerization of thermosetting networks; the blending ratio of 1:3 optimized contact efficiency between the catalysts and feedstock and prevented inefficiencies caused by insufficient active sites.

3.6. Influence of pyrolysis conditions on the composition of pyrolysis gas

3.6.1. Influence of pyrolysis temperature

As shown in Fig. 5(b), the influence of pyrolysis temperature on the composition of pyrolysis gas, and it was obvious that when the pyrolysis temperature was between 400 and 600 °C, the content of CO_2 decreased from 57.79% to 39.66%, and the contents of hydrocarbon gases increased from 26.36% to 37.01%. The proportion of CO_2 decreased significantly with increasing temperature, which was mainly because CO_2 was one of the main components produced from the epoxy resin due to volatilization reactions at lower temperatures. As the temperature increased, the breaking of C–C bonds in the epoxy resin was promoted, generating more hydrocarbon gases CH_4, C_2H_6, C_2H_4, C_3H_6, and C_3H_8. Therefore, the proportion of hydrocarbon gases increased significantly with temperature. Moreover, H_2 increased from 13.84% to 23.34%. These gases reached their highest percentages at 600 °C, indicating that high temperatures promoted deep cracking and dehydrogenation reactions of epoxy resin in the WWTB (Hu et al., 2018).

3.6.2. Influence of pyrolysis time

The influence of pyrolysis time on the composition of pyrolysis gas was shown in Fig. 5(c). H_2 showed a trend of first decreasing and then increasing with pyrolysis time, and reached a maximum percentage of 28.64% at 25 min. CO_2 decreased from 40.57% to 32.01%, and the hydrocarbon gases increased from 31.96% to 39.35%. At the early stage of pyrolysis, CO_2 and H_2 were generated from the surface of epoxy resin through the fracture of the C–O–C bond and the C–H bond. With the increase in pyrolysis time, the

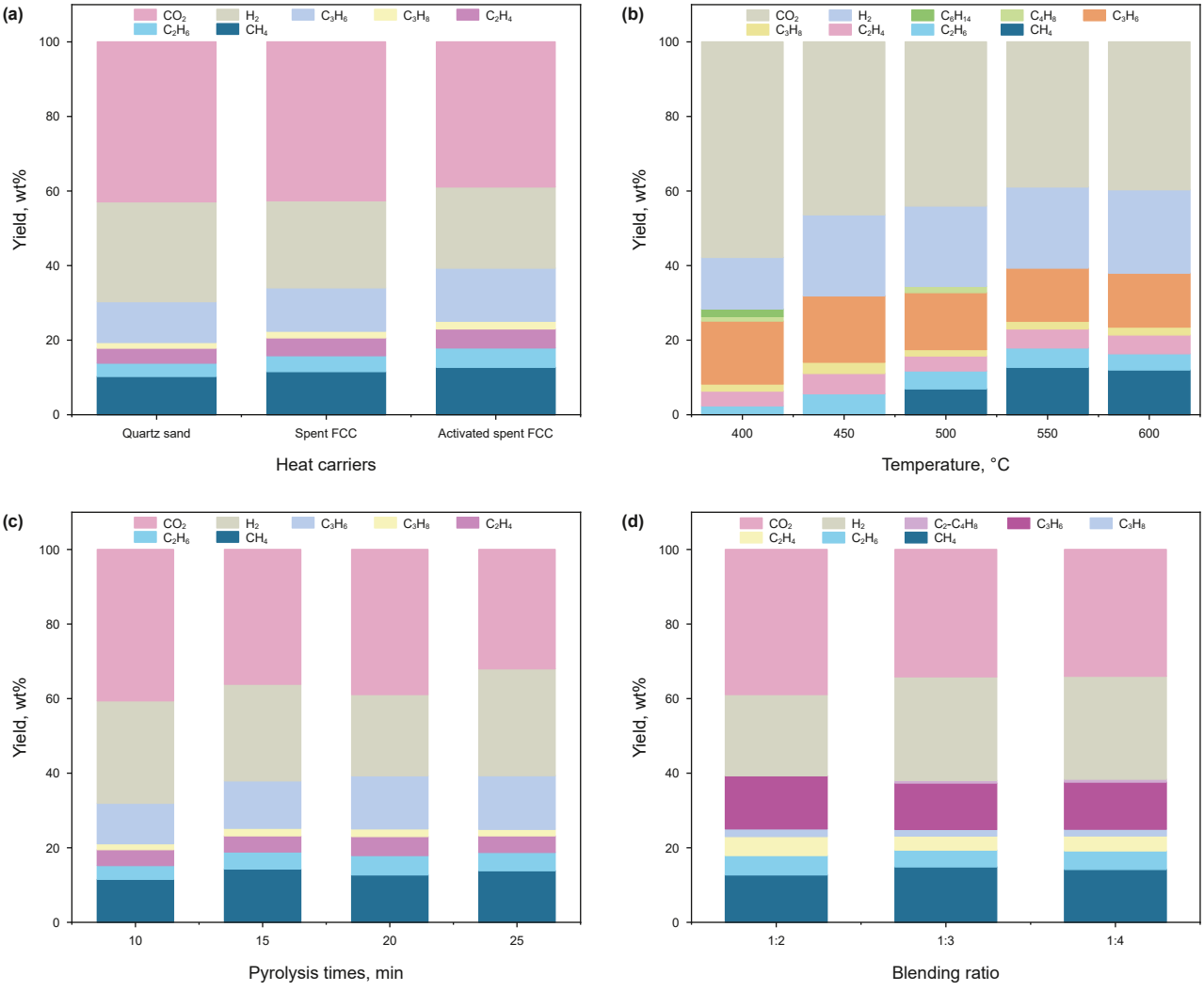


Fig. 5. Influence of pyrolysis gas composition under different **(a)** heat carriers, **(b)** temperature, **(c)** pyrolysis time, **(d)** catalysts blending ratio.

epoxy resin underwent deeper pyrolysis, resulting in an increase in the percentage of hydrocarbon gases (Ge et al., 2023). The percentage of C_3H_6 increased significantly from 10.88% to 14.41%, which was mainly due to the release of the cross-linked structure of the epoxy resin with prolonged pyrolysis, favoring the formation and stabilization of alkene structures. Throughout the pyrolysis process, no C_4H_8 (N), C_4H_8 (I), C_4H_{10}, or C_5 were produced, indicating that the pyrolysis gas was dominated by small-molecule hydrocarbon gases and that the large-molecule hydrocarbon gases were thoroughly pyrolyzed due to the high temperature or extended pyrolysis time (Yun et al., 2015).

3.6.3. Influence of different solid heat carriers

The influence of different solid heat carriers on the composition of pyrolysis gas was shown in Fig. 5(a). The content of C_3H_6 (ring) increased from 10.96% to 14.25% after changing the heat carrier from quartz sand to spent FCC catalysts. This indicated that the acidic sites of the spent FCC catalysts promoted the breakage of C–C bonds, thereby cracking heavy hydrocarbons into small-molecule gases such as C_3H_6, and promoting the formation and stabilization of ring structures (Kongngoen et al., 2023). The proportion of methane increased from 10.27% to 12.72%, and the proportion of ethylene increased from 4% to 5.12%, which further confirmed that the acidic sites of the spent FCC catalysts promoted the deep cracking of epoxy resin in the WWTB.

3.6.4. Influence of different blending ratios on gas composition

The influence of different blending ratios between the WWTB and the spent FCC catalysts on the composition of pyrolysis gas was shown in Fig. 5(d). When the blending ratio was 1:2, the C–O bond and C–C bond of the epoxy resin part started to break, so the proportion of C_2 and C_3 gases was relatively high. At the blending ratio of 1:3, the deep cracking of the epoxy resin occurred, the proportion of C_2 and C_3 gases decreased significantly, and especially the cracking of C_3H_6 was promoted, with its proportion decreasing from 14.25% to 12.63%. At the blending ratio of 1:4, excessive solid heat carrier led to localized uneven heating and carbon accumulation, which weakened the breakage of C–O bonds in epoxy resin and decreased the content of hydrocarbon gases.

3.7. Catalytic performance: selectivity towards total phenolics and phenol

The area normalization method was used to analyze the composition of the pyrolysis oil under various conditions. It was found that the total peak areas value of these fifteen samples of

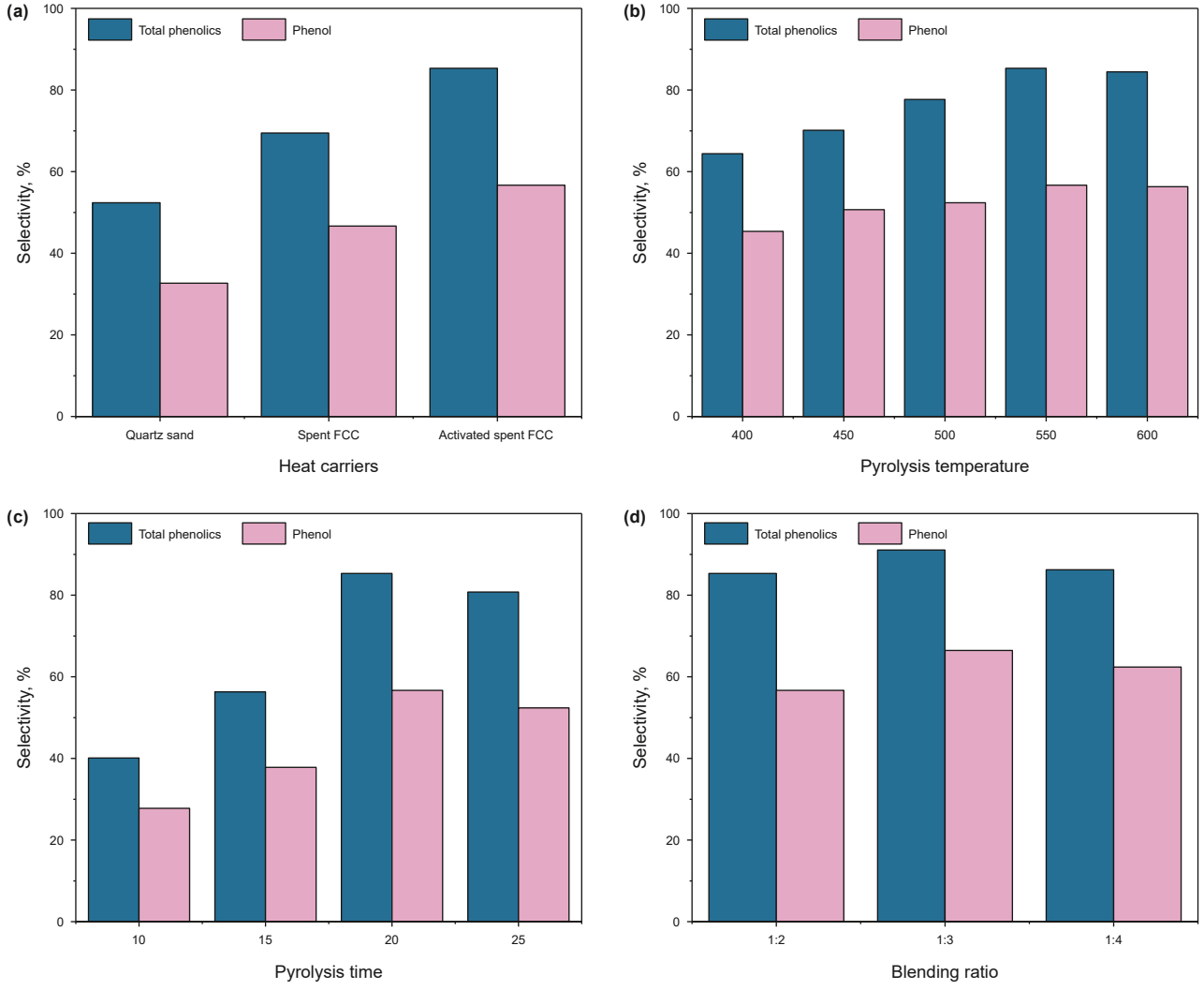
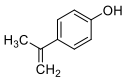
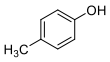
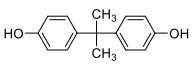
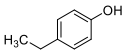
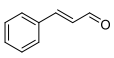


Fig. 6. Influence of total phenolics and phenol selectivity. Different **(a)** heat carriers, **(b)** temperature, **(c)** pyrolysis time, **(d)** catalysts blending ratio.

Table 4
The composition of pyrolysis oil under optimal condition.

Component	Formula	Optimal condition	Structure
Phenol	C_6H_6O	66.47	
4-Isopropenylphenol	$C_9H_{10}O$	12.57	
p-Cresol	C_7H_8O	3.85	
Styrene	C_8H_8	1.80	
BPA	$C_{15}H_{16}O_2$	2.66	
Toluene	C_7H_8	2.13	
Butyraldehyde	C_4H_8O	2.12	
2-Methylphenol	C_7H_8O	1.43	
p-Ethylphenol	$C_8H_{10}O$	1.36	
Benzene	C_6H_6	1.27	
Anisole	C_7H_8O	1.21	
2-Ethylphenol	$C_8H_{10}O$	1.11	
2-Isopropylphenol	$C_9H_{12}O$	1.62	
Cinnamaldehyde	C_9H_8O	0.40	

pyrolysis oil were not significantly different, but the peak area ratios of phenolics, especially that of phenol, were quite different. Therefore, the peak areas ratio of total phenolics and phenol were expressed as selectivity of total phenolics and phenol.

3.7.1. Influence of different heat carriers

The different heat carriers had a significant influence on selectivity of total phenolics and phenol (Fig. 6(a)). When quartz sand was used, the selectivity of total phenolics and phenol were 52.37% and 32.67%, respectively. Replacing quartz sand with the spent FCC catalysts, the selectivity of total phenolics and phenol were 69.47% and 46.66%. The activated spent FCC catalysts resulted in a significant improvement in performance, and achieved selectivity of 85.32% for total phenolics and 56.68% for phenol. This enhancement was directly attributed to the restoration of accessible medium-strength acid sites and improved pore structure through the activation process, which favored selective bond cleavage (e.g., C–O–C in epoxy resins).

3.7.2. Influence of pyrolysis temperature

The influence of temperature on selectivity was investigated using the activated catalysts (Fig. 6(b)). The selectivity of total phenolics and phenol increased with temperature from 400 to 550 °C, reaching the maximum values (85.32% and 56.68%). This trend was consistent with the more complete decomposition of the polymer matrix and the increased activity of acid-catalyzed dealkylation and deoxygenation reactions at higher temperatures. A further increase to 600 °C led to a slight decline in total phenolic selectivity (84.44%), demonstrated that some phenolics began secondary cracking, while phenol selectivity remained nearly constant (56.32%), indicating its relative stability under these conditions.

3.7.3. Influence of pyrolysis time

The influence of the pyrolysis time was shown in Fig. 6(c). At 10 min, the selectivity was low (40.09% total phenolics, 27.78% phenol), which indicated the pyrolysis reaction was incompletely. Extending the reaction time to 20 min maximized selectivity, which confirmed that sufficient pyrolysis time was required for the catalytic reactions. An extension to 25 min, the total phenolics was decreased, so prolong pyrolysis time caused secondary reactions of the phenolics.

3.7.4. Influence of blending ratio

As shown in Fig. 6(d), the blending ratio significantly influenced the composition selectivity, with the highest values (91.07% for total phenolics and 66.47% for phenol) were achieved at blending ratio of 1:3. This ratio represents an ideal balance, providing sufficient catalytic sites for effective cracking and deoxygenation while avoiding excessive secondary reactions or pore blockage that occurred at higher blending ratio (e.g., 1:4).

3.7.5. Comparison

Although a direct quantitative comparison with the literature was precluded by differences in materials and methods, the results were contextualized qualitatively, highlighting the unique findings of this work. For catalytic pyrolysis of WWTB using freshly designed catalysts such as NiO_{10}/Al_2O_3, phenol selectivity was frequently reported in the range of 30%–50% (Li et al., 2024; Yousef et al., 2025). In contrast, the use of the spent FCC catalyst in this manuscript resulted in a significantly higher phenol selectivity of approximately 66.5%. This difference demonstrated the Brønsted acid sites in the spent FCC catalyst for selectively cleaving C–O bonds in epoxy resins, thereby directing the conversion toward valuable monomeric phenols rather than light gases or char. These pyrolysis experiments provided experimental data for the subsequent industrial processing of WWTB and spent FCC catalysts.

3.7.6. Optimal conditions and selectivity trends

The composition of the pyrolysis oil under the optimal condition was shown in Table 4. Systematic optimization demonstrated that the highest selectivity for both total phenolics (91.07%) which included 4-isopropenylphenol, p-cresol, BPA, 2-methylphenol, p-ethylphenol, 2-ethylphenol, 2-isopropylphenol and phenol (66.47%) was achieved. Deviations from these optimal parameters, such as insufficient time or excessive catalysts loading, consistently resulted in decreased selectivity, due to either incomplete pyrolysis or secondary reactions. These results established that precise control over both the catalysts properties and the reaction environment was essential for directing the pyrolysis of WWTB towards the selective production of high-value phenolic chemicals.

4. Conclusion

This study demonstrated a synergistic strategy for the resource recovery of solid wastes through the catalytic pyrolysis of WWTB using spent FCC catalysts in a fluidized-bed reactor. Systematic optimization obtained the optimal conditions (the activated spent

FCC catalysts, 550 °C, 20 min, and a blending ratio of 1:3) and produced the highest pyrolysis oil yield of 28.28 wt%. GC-MS analysis indicated the selectivity towards valuable chemicals with the content of phenolics in the pyrolysis oil reaching 91.07%, among which phenol accounted for 66.47%. The pyrolysis gas had a lot of light hydrocarbons and H_2, offered promising energy-recovery potential. This work demonstrated a strategy with dual environmental and economic advantages by synergistically utilizing two industrial wastes—spent FCC catalyst and WWTB to produce high-value chemical feedstocks.

CRediT authorship contribution statement

Hao-Lun Wang: Supervision, Software, Project administration, Data curation, Conceptualization. **Yue Ma:** Investigation, Funding acquisition, Conceptualization. **Zhi-Jun Fu:** Investigation, Data curation, Writing – original draft. **Lu Gong:** Investigation, Funding acquisition, Conceptualization. **Dong-Ling Xu:** Software, Resources, Methodology. **Ze-Kai Zhang:** Data curation. **Jin-Ke Wang:** Software. **Si-Jia Li:** Software, Data curation. **Feng-Zhi Guo:** Software. **Chang-Tao Yue:** Methodology, Investigation, Funding acquisition.

Declaration of competing interest

The authors declare that they have no known competing financial interests or personal relationships that could have appeared to influence the work reported in this paper.

Supplementary data

Supplementary data to this article can be found online at https://doi.org/10.1016/j.petsci.2026.05.017.

References

Aisien, E.T., Otuya, I.C., Aisien, F.A., 2021. Thermal and catalytic pyrolysis of waste polypropylene plastic using spent FCC catalyst. Environ. Technol. Innovat. 22, 101455. https://doi.org/10.1016/j.eti.2021.101455.

Chen, S., Liu, J., Lin, Z., Lin, S., Li, L., Chen, Y., Evrendilek, F., Li, W., Huang, W., Yang, C., 2025. Atmosphere-dependent pyrolytic transformability of glass fiber/epoxy resin composites in waste wind turbine blades. Chem. Eng. J. 505, 159675. https://doi.org/10.1016/j.cej.2025.159675.

Choi, Y., Wang, S., Yoon, Y.M., Jang, J.J., Kim, D., Ryu, H.-J., Lee, D., Won, Y., Nam, H., Hwang, B., 2024. Sustainable strategy for converting plastic waste into energy over pyrolysis: a comparative study of fluidized-bed and fixed-bed reactors. Energy 286, 129564. https://doi.org/10.1016/j.energy.2023.129564.

de la Puente, G., Klocker, C., Sedran, U., 2002. Conversion of waste plastics into fuels: recycling polyethylene in FCC. Appl. Catal. B Environ. 36 (4), 279–285. https://doi.org/10.1016/S0926-3373(01)00287-9.

Ekici, E., Yildiz, M.J., Kalinowska, M., Wang, J., Yildiz, G., 2025. Co-pyrolysis of waste wind turbine blades in a molten polyolefin medium. J. Anal. Appl. Pyrolysis, 107143. https://doi.org/10.1016/j.jaap.2025.107143.

Ge, L., Li, X., Feng, H., Xu, C., Lu, Y., Chen, B., Li, D., Xu, C., 2023. Analysis of the pyrolysis process, kinetics and products of the base components of waste wind turbine blades (epoxy resin and carbon fiber). J. Anal. Appl. Pyrolysis 170, 105919. https://doi.org/10.1016/j.jaap.2023.105919.

Gu, X., Ma, X., Li, L., Liu, C., Cheng, K., Li, Z., 2013. Pyrolysis of poplar wood sawdust by TG-FTIR and Py–GC/MS. J. Anal. Appl. Pyrolysis 102, 16–23. https://doi.org/10.1016/j.jaap.2013.04.009.

Hamid, S., Niezrecki, C., Eberle, A., 2025. Contextualizing wind turbine blade waste: comparison to other global waste streams. SAMPE J. 61 (3), 16–27. https://doi.org/10.33599/SJ.v61no3.02.

Hu, J., Danish, M., Lou, Z., Zhou, P., Zhu, N., Yuan, H., Qian, P., 2018. Effectiveness of wind turbine blades waste combined with the sewage sludge for enriched carbon preparation through the co-pyrolysis processes. J. Clean. Prod. 174, 780–787. https://doi.org/10.1016/j.jclepro.2017.10.166.

Kabakcı, S.B., Şenlik, A., 2025. End-of-Life wind turbine blades as a resource: a comparative study of pyrolysis and combustion. J. Anal. Appl. Pyrolysis, 107308. https://doi.org/10.1016/j.resconrec.2019.02.039.

Kanduri, P.K., Seethamraju, S., 2023. Effect of process mode on product yields and selectivity in the catalytic co-pyrolysis of peanut shells and polypropylene using spent fluid catalytic cracking (FCC) catalyst. Bioresour. Technol. Rep. 22, 101478. https://doi.org/10.1016/j.biteb.2023.101478.

Kongngoen, P., Phetwarotai, W., Assabumrungrat, S., Phusunti, N., 2023. Possible use of spent FCC catalyst for upgrading of wax from the pyrolysis of plastics to liquid fuel. J. Anal. Appl. Pyrolysis 173, 106076. https://doi.org/10.1016/j.jaap.2023.106076.

Li, J.H., Jiang, H., Chen, W.W., Wu, Y.C., Xu, M.X., Di, J.Y., Li, W., Lu, Q., 2024. Selective production of phenol from the end-of-life wind turbine blade through catalytic pyrolysis. Fuel 378, 132877. https://doi.org/10.1016/j.fuel.2024.132877.

Li, J., Yu, W., Gao, J., 2025. Separation of polycyclic aromatic hydrocarbons by solvent screening assisted extractive distillation from FCC diesel. Chin. J. Chem. Eng. https://doi.org/10.1016/j.cjche.2025.09.001.

Lichtenegger, G., Rentizelas, A.A., Trivyza, N., Siegl, S., 2020. Offshore and onshore wind turbine blade waste material forecast at a regional level in Europe until 2050. Waste Manag. 106, 120–131. https://doi.org/10.1016/j.wasman.2020.03.018.

Liu, P., Barlow, C.Y., 2017. Wind turbine blade waste in 2050. Waste Manag. 62, 229–240. https://doi.org/10.1016/j.wasman.2017.02.007.

Liu, H.T., Wang, J.J., Xie, F.M., Li, Y.C., Li, H.Y., Liu, H.Y., Yue, Y.Y., Mi, X.T., Gao, X.H., Liu, H.H., 2023. Hydrothermally stable mesoporous aluminosilicates as superior FCC catalyst: from laboratory to refinery. Pet. Sci. 20 (3), 1903–1908. https://doi.org/10.1016/j.petsci.2022.11.028.

Lu, G., Lu, X., Liu, P., 2020. Reactivation of spent FCC catalyst by mixed acid leaching for efficient catalytic cracking. J. Ind. Eng. Chem. 92, 236–242. https://doi.org/10.1016/j.jiec.2020.09.011.

Ma, Z., Qu, L., Zhou, P., Song, Z., Zhao, X., Wang, W., 2025. A review of research on the resource utilization of pyrolysis of decommissioned wind turbine blades. Energies 18 (4), 782. https://doi.org/10.3390/en18040782.

Marschall, M.S., Seifert, M., Hauck, M., Busse, O., Weigand, J.J., 2025. Zeolite synthesis using recycled silicon and aluminum components from spent FCC catalysts. Waste Manag. 202, 114817. https://doi.org/10.1016/j.wasman.2025.114817.

Mavukwana, A.-e., Burra, K.G., Sempuga, C., Castaldi, M., Gupta, A.K., 2024. Effect of spent fluid catalytic cracking (FCC) catalyst on syngas production from pyrolysis and CO2-assisted gasification of waste tires. Fuel 355, 129446. https://doi.org/10.1016/j.fuel.2023.129446.

Mishra, R.R., Rana, P.H., Parikh, P.A., 2025. Influence of catalyst acidity of spent FCC catalyst and TiO2 on product distribution in microwave assisted LDPE cracking. J. Indian Chem. Soc., 101873 https://doi.org/10.1016/j.jics.2025.101873.

Nistratov, A.V., Klimenko, N.N., Pustynnikov, I.V., Vu, L.K., 2022. Thermal regeneration and reuse of carbon and glass fibers from waste composites. Emerg. Sci. J. 6 (5), 967–984. https://doi.org/10.28991/esj-2022-06-05-04.

Passamonti, F.J., Sedran, U., 2012. Recycling of waste plastics into fuels. LDPE conversion in FCC. Appl. Catal. B Environ. 125, 499–506. https://doi.org/10.1016/j.apcatb.2012.06.020.

Ren, Q.Q., Lei, Z.W., Hu, S., Ding, Y., He, L.M., Su, S., Wang, Y., Jiang, L., Xu, J., Xiang, J., 2023. Novel photothermal pyrolysis on waste fan blade to generate bisphenol A. J. Anal. Appl. Pyrolysis 169, 105828. https://doi.org/10.1016/j.jaap.2022.105828.

Salvilla, J.N.V., Yang, S., Liu, Q., Xie, Z., Chen, Z., Song, H., Zhang, L., 2025. Elucidating the role of carbon dioxide (CO_2) in the transformation of hydrogen cyanide (HCN) during the regeneration of spent fluid catalytic cracking (FCC) catalysts. J. Environ. Manag. 389, 126165. https://doi.org/10.1016/j.jenvman.2025.126165.

Teng, H., Li, S., Cao, Z., Li, S., Li, C., Ko, T.J., 2023. Carbon fiber composites for large-scale wind turbine blades: applicability study and comprehensive evaluation in China. J. Mar. Sci. Eng. 11 (3), 624. https://doi.org/10.3390/jmse11030624.

Tian, X., Han, S., Wang, K., Shan, T., Li, Z., Li, S., Wang, C., 2022. Waste resource utilization: spent FCC catalyst-based composite catalyst for waste tire pyrolysis. Fuel 328, 125236. https://doi.org/10.1016/j.fuel.2022.125236.

Wang, B.L., Wang, X.Y., Xu, N.D., Shen, Y.B., Lu, F., Liu, Y.Y., Huang, Y.D., Hu, Z., 2021. Recycling of carbon fibers from unsaturated polyester composites via a hydrolysis-oxidation synergistic catalytic strategy. Compos. Sci. Technol. 203, 108589. https://doi.org/10.1016/j.compscitech.2020.108589.

Wang, P., Qiao, L., Wang, W., Yu, J., 2023. Catalytic pyrolysis of waste composite plastics with waste FCC catalyst. J. Energy Inst. 110, 101338. https://doi.org/10.1016/j.joei.2023.101338.

Wang, B., Yan, Y., Zhou, X., Su, H., Zhang, H., Zhang, J.N., Xu, J., Pan, Q., Yan, W., 2024. Mild activation of spent fluid catalytic cracking (FCC) catalysts for the pilot synthesis of zeolite a with commercial quality and excellent Co^{2+} removal ability. Chem. Eng. J. 490, 151733. https://doi.org/10.1016/j.cej.2024.151733.

Xiang, H., Wang, G., Wang, C., Zhang, Q., Shi, Z., Ekananda, R., Gamar, I., Zhang, J., Chen, J., Wang, R., 2025. Efficient recovery of nickel from spent FCC catalysts by sulfation roasting-leaching. Waste Manag. 205, 115041. https://doi.org/10.1016/j.wasman.2025.115041.

Xu, D., Zhang, X., Jing, T., 2019. Research on key technologies of recycling and utilization of waste thermosetting composites such as waste wind blades in

China's wind power industry. Environ. Protect. 47 (20), 54–56. https://doi.org/10.14026/j.cnki.0253-9705.2019.20.013.
Xu, Y., Wang, F., Liang, D., Lv, G., He, F., Xue, S., 2025. A comparative pyrolysis study of different waste wind turbine blade parts: kinetics, product distribution and evolution, and economics. Waste Manag. 200, 114782. https://doi.org/10.1016/j.wasman.2025.114782.
Yousef, S., Eimontas, J., Zakarauskas, K., Stasiulaitiene, I., Striūgas, N., Tuckute, S., 2025. Catalytic pyrolysis of wind turbine blades waste for plasticizers recovery and its life cycle assessment. J. Environ. Manag. 395, 127690. https://doi.org/10.1016/j.jenvman.2025.127690.
Yun, Y.M., Seo, M.W., Ra, H.W., Koo, G.H., Oh, J.S., Yoon, S.J., Kim, Y.K., Lee, J.G., Kim, J.H., 2015. Pyrolysis characteristics of glass fiber-reinforced plastic (GFRP) under isothermal conditions. J. Anal. Appl. Pyrolysis 114, 40–46. https://doi.org/10.1016/j.jaap.2015.04.013.
Zhang, B., Zhang, S., Yang, Z., Liu, W., Wu, B., Huang, M., Liu, B., 2024. Pyrolysis process and products characteristics of glass fiber reinforced epoxy resin from waste wind turbine blades. Compos. B Eng. 287, 111803. https://doi.org/10.1016/j.compositesb.2024.111803.